Large Displacement Analysis of Elasto-Plastic Thin-Walled Frames

Part I: Formulation and Implementation

B.A. Izzuddin[1] and D. Lloyd Smith[2]

ABSTRACT

This paper presents a new formulation for the large displacement analysis of thin-walled frames taking into account the effects of elasto-plastic material behaviour. The proposed formulation is derived in an Eulerian (convected) local system which allows relatively simple strain-displacement relationships to be used. Furthermore, the formulation employs the fibre approach for representing the spread of plasticity over a general open cross-section, and is capable of modelling initial imperfections, residual stresses and the Wagner effect. In accounting for material plasticity effects, consideration is given to the interaction between normal stresses and shear stresses due to twisting. Since the shear strain is directly related to the rate of twist, the shear stress in the yield function is replaced by an equivalent contribution to the cross-sectional torque, which leads to considerable computational advantages. The present paper describes the formulation details and the implementation of material plasticity effects for kinematic and isotropic strain-hardening, whereas the companion paper provides a number of verification and application examples.

KEYWORDS

Thin-walled frames. Large displacements. Elasto-plastic analysis. Lateral-torsional buckling.

---

[1] Lecturer in Engineering Computing, Department of Civil Engineering, Imperial College, London SW7 2BU, U.K.

[2] Reader in Structural Mechanics, Department of Civil Engineering, Imperial College, London SW7 2BU, U.K.

INTRODUCTION

The past few years have witnessed intensive research efforts directed towards the development of advanced nonlinear analysis tools which are capable of predicting the response of various structural forms in the large displacement inelastic domain. Several researchers, however, have been concerned with the development of analysis methods which provide accurate predictions at minimal computational cost, since the nonlinear analysis of realistic structures can prove to be prohibitively expensive, even using the most powerful of computers.

The earliest attempts at understanding the behaviour of thin-walled structures were focused on the investigation of lateral torsional buckling. With the assumption of elastic response, mathematical expressions were derived for the buckling loads of beams with various boundary conditions (Bleich, 1952; Allen and Bulson, 1980). Barsoum and Gallagher (1970) introduced a numerical approach for elastic buckling calculations based on the finite element method, allowing the effects of general boundary conditions to be investigated. Trahair and Kitipornchai (1972) considered the elasto-plastic lateral torsional buckling of I-beams subject to uniform bending moment; for this, they reverted to the mathematical expressions for elastic buckling, in which they then replaced the elastic Young's and shear modulii by tangent values so as to account for the spread of plasticity within the cross-section. While the buckling analysis was simplified by the consideration of a uniform bending moment, assumptions had to be made regarding the value of the shear tangent modulus, and complexities were introduced by residual stresses causing a change in the position of the shear centre upon yielding. Nethercot (1975) combined finite element approximation (Barsoum and Gallagher, 1970) with the tangent modulus approach (Trahair and Kitipornchai, 1972) to study the inelastic lateral torsional buckling of I-beams under non-uniform bending moment. Recently, Pi and Trahair (1992) included the effects of pre-buckling deflections on the lateral torsional buckling of beam-columns with a mono-symmetric cross-section.

With the advent of powerful computers, large displacement analysis methods became the focus of research efforts, promising the ability to predict the buckling, as well as the post-buckling, response of structures. In the context of framed structures, initial efforts were concerned with the development of one-dimensional finite element approaches for modelling large displacements and finite rotations in the absence of warping effects, three main approaches being identified: Total Lagrangian, Updated Lagrangian and Eulerian. In the Total Lagrangian approach, system variables are referred to the initial position of the element, leading to complex strain-displacement relationships (Mallet and Marcal, 1968; El-Zanaty and Murray, 1983). In the Updated Lagrangian approach, system quantities are referred incrementally to the last known equilibrium configuration, which results in simpler strain-displacement relationships, although there are restrictions on the size of the incremental step (Wen and Rahimzadeh, 1983). In the Eulerian approach, system quantities are referred to the current unknown configuration (Oran, 1973), allowing linear strain-displacement relationships to be used in the local system, with geometric nonlinearities introduced through transformations between the global and local system (Izzuddin and Elnashai, 1993-a).

The large displacement analysis of elastic thin-walled frames required further developments in which warping freedoms had to be incorporated to enforce cross-sectional displacement continuity between adjacent elements in the case of non-uniform warping. Most of these developments were based on the Updated Lagrangian approach (Bazant and El Nimeiri, 1973; Chan and Kitipornchai, 1987; Conci and Gattass, 1990-a; Chen and Blandford, 1991), although the extension of an Eulerian approach to thin-walled frames has been recently proposed by the first author (Izzuddin, 1995).

In addition to the above developments, realistic large displacement analysis of framed structures required incorporation of the effects of material nonlinearity. Meek and Loganathan (1990) modelled material elasto-plasticity in terms of uniaxial normal stresses, and later Meek and Lin (1990) included the interaction of normal and shear stresses in the plastic range, although in both cases only closed cross-sections were considered and warping effects were ignored. A similar approach, founded on uniaxial stresses, was set out by Izzuddin and

Elnashai (1993-b) in the context of adaptive elasto-plastic analysis of steel frames. For thin-walled frames, Epstein *et al.* (1978) proposed an elasto-plastic formulation based on a tangent modulus approach; but it neither accounts for strain reversals nor for plastic interaction between shear and normal stresses. Conci and Gattass (1990-b) adopted a plastic-hinge approach and commented on the difficulty of establishing the yield condition as a relationship between generalised cross-sectional stresses. Hasegawa *et al.* (1987) considered plasticity in terms of material stresses, although the interaction between shear and normal stresses was simplified by the assumption that the tangent shear modulus is proportional to the normal tangent modulus. The most recent and complete work is that of Pi and Trahair (1994), where a Total Lagrangian approach was used, and a von Mises interaction with isotropic work hardening was assumed between the shear and normal stresses in the plastic range. However, the proposed method was based on complex strain-displacement relationships necessitated by the Total Lagrangian approach, it considered only collinear beam-column systems, and it imposed excessive computational requirements in material plasticity calculations.

This paper presents a new one-dimensional formulation for the large displacement analysis of elasto-plastic frames composed of members with any thin-walled open cross-section. The proposed formulation is derived in a local Eulerian system (Izzuddin, 1995), thereby allowing simplified strain-displacement relationships to be used. The spread of plasticity is modelled with the new formulation through the use of monitoring points for stresses and strains over the cross-section and two Gauss points along the element length. In addition, the formulation accounts for initial twist imperfections, residual stresses and the Wagner effect (Goto and Chen, 1989). The von Mises yield criterion is employed to model the plastic interaction of shear stresses (arising from torsion) and normal stresses, where both isotropic and kinematic strain hardening are considered. In this context, it is shown that considerable computational benefits are achieved by replacing the shear stress in the yield condition with an equivalent contribution to the cross-sectional torque. The paper proceeds by describing the Eulerian approach and providing the cubic formulation details, the companion paper (Izzuddin and

Lloyd Smith, 1995) presenting verification examples and applications for the proposed formulation.

EULERIAN APPROACH

The proposed elasto-plastic formulation is derived in a local Eulerian system (Izzuddin, 1995), where the element displacements are referred to the element chord in the current (unknown) configuration, as shown in Fig. 1. Vectors $({}^{1}_{y}c, {}^{1}_{z}c)$ and $({}^{2}_{y}c, {}^{2}_{z}c)$ represent the cross-sectional orientation at the two element nodes, whereas vector $({}_{x}c)$ represents the current element chord (Izzuddin and Elnashai, 1993-a). In order to facilitate one-dimensional modelling, the following assumptions are made regarding the displacements over a general open cross-section:

1. plane sections remain plane in the absence of cross-sectional warping,

2. in-plane shear strains at the mid-plane of component plates, as well as the out-of-plane shear strains, are zero, and

3. the projection of the displaced cross-section on a plane perpendicular to the axial direction is always of the same shape and size; that is cross-sectional distortion is ignored.

With these assumptions, the strain state of a cross-section can be completely defined in terms of four reference line displacements $(u_g, v_g, w_g, \alpha_g)$, shown in Fig. 2 for point (O), and their derivatives. Two cross-sectional reference systems are defined in the deflected configuration; the first $(\bar{y},\bar{z})$ represents the cross-section axes in the absence of twist imperfection (α^{i}_{g}), whereas the second (y,z) is the material reference system following the deflected and imperfect shape. A direct mapping exists between the two systems, which can be expressed for small twist imperfection by the following:

$$\bar{y} = y + v^{i} \qquad (1.a)$$

$$\bar{z} = z + w^i \tag{1.b}$$

in which,

$$v^i = -z\,\alpha_g^i \tag{2.a}$$

$$w^i = y\,\alpha_g^i \tag{2.b}$$

Whilst accurate nonlinear analysis usually requires higher order terms in nonlinear strain-displacement relationships, the Eulerian approach allows terms involving the transverse displacements (v_g, w_g) and their first derivatives with respect to (x) (v_g', w_g') to be ignored when several elements are used to represent one member. As illustrated in Fig. 3 for uniform curvature, the maximum transverse displacement is inversely proportional to square of the number of elements, whereas the maximum value of the first derivative is inversely proportional to the number of elements. Therefore, as the number of elements increases, the values of transverse displacements and their first derivatives become so small that terms involving these variables can be ignored. In addition, the use of a number of elements allows transverse imperfections to be readily modelled by offsetting initial nodal coordinates from the member chord; this information, however, is not sufficient to prescribe the twist imperfection which is specified for each element by a separate function (α_g^i).

The three assumptions stated previously can be used to express the cross-sectional displacements (u,v,w) of point (P) in terms of the four reference line displacements $(u_g, v_g, w_g, \alpha_g)$, as shown in Fig. 2. For small transverse displacements (v_g, w_g), the axial displacement (u) and the transverse displacements (v,w) in the direction of the cross-sectional axes $({}_y^1c, {}_z^1c)$ at node (1) are given by:

$$u = u_g - \bar{y}\,v_g' - \bar{z}\,w_g' + \Phi\alpha_g' \tag{3.a}$$

$$v = v_g - (\bar{z} + w_g)\alpha_g \tag{3.b}$$

$$w = w_g + (\bar{y} + v_g)\alpha_g \tag{3.c}$$

where (Φ) is a warping function of (y,z) which can be readily established for any thin-walled open cross-section (Izzuddin, 1995). The normal strain (ε_x) can be related to the cross-sectional displacements by the second order expression:

$$\varepsilon_x = \frac{\partial u}{\partial x} + \frac{1}{2}\left[\left(\frac{\partial v}{\partial x} + \frac{\partial v^i}{\partial x}\right)^2 - \left(\frac{\partial v^i}{\partial x}\right)^2 + \left(\frac{\partial w}{\partial x} + \frac{\partial w^i}{\partial x}\right)^2 - \left(\frac{\partial w^i}{\partial x}\right)^2\right] \tag{4}$$

in which (v^i, w^i) are the transverse cross-sectional displacements due to twist imperfection given by (2). Considering (2)-(4), the normal strain can be expressed as a nonlinear function of the reference line displacements (u_g, v_g, w_g, α_g) and their derivatives. If all terms of (v_g, w_g, v'_g, w'_g) are ignored, as allowed by the Eulerian approach, and terms of other displacement derivatives up to the second order are included, the following simplified expression for (ε_x) is obtained:

$$\varepsilon_x = u'_g - y\left(v''_g + \alpha^i_g w''_g\right) - z\left(w''_g - \alpha^i_g v''_g\right) + \Phi\alpha''_g + (y^2 + z^2)\left(\frac{\alpha'^2_g}{2} + \alpha'^i_g \alpha'_g\right) \tag{5}$$

where the last quadratic term is necessary for modelling the Wagner effect (Goto and Chen, 1989). Other forms of geometric nonlinearity, including the beam-column effect and flexural-torsional coupling, are modelled effectively by subdividing each member into several elements.

The only other strain required by this formulation is the in-plane shear strain, which can be shown to vary linearly through the thickness of component plates with a zero mid-plane value (Izzuddin, 1995):

$$\gamma_{x\hat{y}} = \frac{\partial u}{\partial \hat{y}} + \frac{\partial \hat{v}}{\partial x} = \left(\frac{\partial \Phi}{\partial \hat{y}} - \hat{z}\right)\alpha'_g \Rightarrow$$

$$\gamma_{x\hat{y}} = -2\hat{z}\,\alpha'_g \tag{6}$$

where ($\hat{y}, \hat{z}$) is the local reference system for a component plate, as shown in Fig. 4.

CUBIC FORMULATION

The proposed formulation employs eight local degrees of freedom, including two warping freedoms, with the deflected centroidal axis chosen as the element reference line, as shown in Fig. 5:

$$ {}_{c}u = \left\langle \theta_{1y}, \theta_{1z}, \theta_{2y}, \theta_{2z}, \Delta, \theta_{T}, \theta'_{1}, \theta'_{2} \right\rangle^{T} \tag{7} $$

Cubic shape functions are used for the transverse reference line displacements (v_g, w_g) and angle of twist (α_g), whereas a linear shape function is employed for the axial displacement (u_g):

$$ u_g(x) = \Delta\left(\frac{x}{L}\right) \tag{8.a} $$

$$ v_g(x) = \left(L\left\{\theta_{1y} + \theta_{2y}\right\}\right)\left(\frac{x}{L}\right)^3 - \left(L\left\{2\theta_{1y} + \theta_{2y}\right\}\right)\left(\frac{x}{L}\right)^2 + \theta_{1y}x \tag{8.b} $$

$$ w_g(x) = \left(L\left\{\theta_{1z} + \theta_{2z}\right\}\right)\left(\frac{x}{L}\right)^3 - \left(L\left\{2\theta_{1z} + \theta_{2z}\right\}\right)\left(\frac{x}{L}\right)^2 + \theta_{1z}x \tag{8.c} $$

$$ \alpha_g(x) = \left(L\left\{\theta'_1 + \theta'_2\right\} - 2\theta_T\right)\left(\frac{x}{L}\right)^3 - \left(L\left\{2\theta'_1 + \theta'_2\right\} - 3\theta_T\right)\left(\frac{x}{L}\right)^2 + \theta'_1 x \tag{8.d} $$

where (L) is the element length.

Any imperfection (α_g^i) in the angle of twist is assumed to vary according to a cubic function, the terms of which are determined from values of twist imperfection (θ_1^i, θ_2^i) and the rates of twist imperfection $(\theta_1'^i, \theta_2'^i)$ at the two element nodes:

$$ \alpha_g^i(x) = \left(L\left\{\theta_1'^i + \theta_2'^i\right\} - 2\left\{\theta_2^i - \theta_1^i\right\}\right)\left(\frac{x}{L}\right)^3 - \left(L\left\{2\theta_1'^i + \theta_2'^i\right\} - 3\left\{\theta_2^i - \theta_1^i\right\}\right)\left(\frac{x}{L}\right)^2 + $$

$$ \theta_1'^i x + \theta_1^i \tag{9} $$

For the numerical integration of the virtual work equation, two Gauss points are used; their location is given by :

$$ {}_{g}\mathrm{x} = \left\langle \frac{\mathrm{L}}{6}\left(3-\sqrt{3}\right), \frac{\mathrm{L}}{6}\left(3+\sqrt{3}\right) \right\rangle^{\mathrm{T}} \tag{10} $$

Although more Gauss points could be employed for more accurate numerical integration over the element length, the use of two integration points for an element is more computationally efficient. Furthermore, since several elements are required to model sufficiently accurately the nonlinear response of one member, the numerical integration over the member length is undertaken with the benefit of a considerable number of Gauss points, and hence accuracy is not compromised. At each Gauss point, the general open cross-section is discretised into monitoring areas where material strains and stresses are evaluated and used to determine the element end forces, as discussed hereafter.

Cross-Sectional Response

With the shape functions for the reference line displacements defined, the distribution of normal and shear strains over the cross-section can be determined according to (5) and (6). For this purpose, a (6×2) matrix of generalised strains $({}_{s}\mathrm{u})$ at the two Gauss points is defined:

$$ {}_{s}\mathrm{u} = \begin{bmatrix} \mathrm{u}'_{g}({}_{g}\mathrm{x}_1) & \mathrm{u}'_{g}({}_{g}\mathrm{x}_2) \\ \mathrm{v}''_{g}({}_{g}\mathrm{x}_1) + \alpha^{\mathrm{i}}_{g}({}_{g}\mathrm{x}_1)\,\mathrm{w}''_{g}({}_{g}\mathrm{x}_1) & \mathrm{v}''_{g}({}_{g}\mathrm{x}_2) + \alpha^{\mathrm{i}}_{g}({}_{g}\mathrm{x}_2)\,\mathrm{w}''_{g}({}_{g}\mathrm{x}_2) \\ \mathrm{w}''_{g}({}_{g}\mathrm{x}_1) - \alpha^{\mathrm{i}}_{g}({}_{g}\mathrm{x}_1)\,\mathrm{v}''_{g}({}_{g}\mathrm{x}_1) & \mathrm{w}''_{g}({}_{g}\mathrm{x}_2) - \alpha^{\mathrm{i}}_{g}({}_{g}\mathrm{x}_2)\,\mathrm{v}''_{g}({}_{g}\mathrm{x}_2) \\ \alpha''_{g}({}_{g}\mathrm{x}_1) & \alpha''_{g}({}_{g}\mathrm{x}_2) \\ \alpha'^{2}_{g}({}_{g}\mathrm{x}_1)/2 + \alpha'^{\mathrm{i}}_{g}({}_{g}\mathrm{x}_1)\alpha'_{g}({}_{g}\mathrm{x}_1) & \alpha'^{2}_{g}({}_{g}\mathrm{x}_2)/2 + \alpha'^{\mathrm{i}}_{g}({}_{g}\mathrm{x}_2)\alpha'_{g}({}_{g}\mathrm{x}_2) \\ \alpha'_{g}({}_{g}\mathrm{x}_1) & \alpha'_{g}({}_{g}\mathrm{x}_2) \end{bmatrix} \tag{11} $$

which can be readily established in terms of the local displacements and twist imperfections using (8) and (9).

The integration of the virtual work equation is performed numerically using the two aforementioned Gauss points over the element length and a number of monitoring areas over the cross-section, as shown in Fig. 6 for a channel section. The values of the normal strain (ε_x) and shear strain ($\gamma_{x\hat{y}}$) can be determined at the centre of each monitoring area once the generalised strains ($_s u$) are calculated. However, since the shear strain is simply related to the rate of twist according to (6), the shear state within a monitoring area can be better represented by a rate of twist generalised strain (ξ), identical to (α'_g) evaluated at the Gauss point. This approach has a considerable computational advantage in that the integration of the virtual work equation does not require a fine discretisation over the thickness of component plates, even allowing for only one monitoring area to be used over the plate thickness, albeit at a slight loss in accuracy. Therefore, the strain state ($e_{g,m}$) of monitoring area (m) at Gauss point (g) is defined by the normal strain (ε_x) at the centre of the area and the rate of twist (ξ); it is obtained from the generalised strain matrix ($_s u$) as follows:

$$e_{g,m} = \begin{Bmatrix} \varepsilon_x \\ \\ \xi \end{Bmatrix} \tag{12.a}$$

$$e_{g,m,i} = \sum_{j=1}^{6} d_{m,i,j}\ {}_s u_{j,g} \qquad (i = 1,2) \tag{12.b}$$

where,

$$d_m = \begin{bmatrix} 1 & -y_m & -z_m & \boldsymbol{\Phi}_m & y_m^2 + z_m^2 & 0 \\ 0 & 0 & 0 & 0 & 0 & 1 \end{bmatrix} \tag{13}$$

in which,

(y_m, z_m) : cross-sectional coordinates of monitoring area (m) (Fig. 6)

($\boldsymbol{\Phi}_m$) : value of warping function $\Phi(y,z)$ for monitoring area (m).

The stress state ($s_{g,m}$) of monitoring area (m) at Gauss point (g) is defined by a normal stress (σ_x) at the centre of the area and a twisting moment per unit area (ψ):

$$s_{g,m} = \begin{Bmatrix} \sigma_x \\ \\ \psi \end{Bmatrix} \tag{14}$$

The determination of the stress state ($s_{g,m}$) corresponding to the strain state ($e_{g,m}$) is performed in accordance with the material law, as discussed in a later section.

The cross-sectional generalised stresses ($_sf$) corresponding to the generalised strains ($_su$) at the two Gauss points can now be obtained from the stress states of all the monitoring areas:

$$_sf_{j,g} = \sum_{m=1}^{n} \sum_{i=1}^{2} A_m \, d_{m,i,j} \, s_{g,m,i} \qquad (j = 1,6),(g = 1,2) \tag{15}$$

where,

A_m : area of monitoring area (m)

n : total number of monitoring areas over a cross-section.

Local Element Response

The proposed cubic formulation has eight local forces ($_cf$) corresponding to the local freedoms ($_cu$), with the last two terms corresponding to bimoments at the two element nodes:

$$_cf = \left\langle M_{1y}, M_{1z}, M_{2y}, M_{2z}, F, M_T, B_1, B_2 \right\rangle^T \tag{16}$$

The local forces can be determined from the virtual work equation, which is integrated numerically over the two Gauss points and the cross-sectional monitoring areas:

$$_cf_k \, \delta_c u_k = \int_0^L \int_A \left(\sigma_x \, \delta\varepsilon_x + \tau_{x\hat{y}} \, \delta\gamma_{x\hat{y}} \right) dA \, dx = \frac{L}{2} \sum_{g=1}^{2} \sum_{m=1}^{n} \sum_{i=1}^{2} A_m \, s_{g,m,i} \, \delta e_{g,m,i} \tag{17}$$

Considering (12) and (15) in conjunction with (17), the virtual work equation can be expressed in terms of generalised stresses and strains:

$$ {}_{c}f_{k}\ \delta_{c}u_{k} = \frac{L}{2}\sum_{g=1}^{2}\sum_{j=1}^{6} {}_{s}f_{j,g}\ \delta_{s}u_{j,g} \tag{18} $$

Therefore, the local forces can be obtained from the generalised cross-sectional stresses:

$$ {}_{c}f_{k} = \frac{L}{2}\sum_{g=1}^{2}\sum_{j=1}^{6}\frac{\partial_{s}u_{j,g}}{\partial_{c}u_{k}}\ {}_{s}f_{j,g} \tag{19.a} $$

or,

$$ {}_{c}f_{k} = \sum_{g=1}^{2}\sum_{j=1}^{6} {}_{c}T_{j,g,k}\ {}_{s}f_{j,g} \qquad (k=1,8) \tag{19.b} $$

where $({}_{c}T)$ is a (6×2×8) array, obtained from (8), (9) and (11) and given in Appendix A, representing the weighted first derivatives of generalised strains with respect to local displacements.

The proposed formulation is implemented within an iterative procedure for the solution of the nonlinear system of governing equations; these require the determination of a local tangent stiffness matrix $({}_{c}k)$, defined as:

$$ {}_{c}k_{k,q} = \frac{\partial_{c}f_{k}}{\partial_{c}u_{q}} \qquad (k=1,8),\ (q=1,8) \tag{20} $$

With reference to (19), the local tangent stiffness matrix can be expressed as a transformation of the generalised cross-sectional tangent stiffness at the two Gauss points:

$$ {}_{c}k_{k,q} = \sum_{g=1}^{2}\sum_{j=1}^{6}\left({}_{c}T_{j,g,k}\ \frac{\partial_{s}f_{j,g}}{\partial_{c}u_{q}} + \frac{\partial_{c}T_{j,g,k}}{\partial_{c}u_{q}}\ {}_{s}f_{j,g}\right) \Rightarrow $$

$$ {}_{c}k_{k,q} = \sum_{g=1}^{2}\sum_{j=1}^{6}\left(\left(\frac{2}{L}\right)\sum_{h=1}^{6} {}_{c}T_{j,g,k}\ {}_{s}k_{j,h,g}\ {}_{c}T_{h,g,q} + \frac{\partial_{c}T_{j,g,k}}{\partial_{c}u_{q}}\ {}_{s}f_{j,g}\right) \tag{21.a} $$

where,

$$ {}_{s}k_{j,h,g} = \frac{\partial_{s}f_{j,g}}{\partial_{s}u_{h,g}} \qquad (j=1,6),\ (h=1,6) \tag{21.b} $$

The generalised tangent stiffness matrix $({}_{s}k)$ can be related to the values of the material tangent modulus matrix $({}_{t}E)$ over the cross-sectional monitoring areas by:

$$ {}_{s}k_{j,h,g} = \sum_{m=1}^{n} \sum_{i=1}^{2} \sum_{p=1}^{2} A_m \, d_{m,i,j} \, {}_{t}E_{g,m,i,p} \, d_{m,p,h} \tag{22} $$

where,

$$ {}_{t}E_{g,m} = \begin{bmatrix} \dfrac{\partial \sigma_x}{\partial \varepsilon_x} & \dfrac{\partial \sigma_x}{\partial \xi} \\ \dfrac{\partial \psi}{\partial \varepsilon_x} & \dfrac{\partial \psi}{\partial \xi} \end{bmatrix} \tag{23.a} $$

or,

$$ {}_{t}E_{g,m,i,p} = \frac{\partial s_{g,m,i}}{\partial e_{g,m,p}} \qquad (i = 1,2), \, (p = 1,2) \tag{23.b} $$

The determination of the material tangent modulus matrix $({}_{t}E)$ is performed in accordance with the material constitutive law, as detailed in the following section.

In equation (21.a), the second term may be further developed by noting that:

$$ \frac{\partial \, {}_{c}T_{j,g,k}}{\partial \, {}_{c}u_{q}} = \frac{L}{2} \, \frac{\partial^2 {}_{s}u_{j,g}}{\partial \, {}_{c}u_{k} \, \partial \, {}_{c}u_{q}} \tag{24} $$

It will be found from (11) that only the $({}_{s}u_{5,g})$ terms possess non-zero values of the desired second order derivatives. Evaluating these derivatives and substituting into (21.a) produces the result:

$$ {}_{c}k_{k,q} = \left(\frac{2}{L} \right) \left(\sum_{g=1}^{2} \sum_{j=1}^{6} \sum_{h=1}^{6} {}_{c}T_{j,g,k} \; {}_{s}k_{j,h,g} \; {}_{c}T_{h,g,q} + \sum_{g=1}^{2} {}_{c}T_{6,g,k} \; {}_{s}f_{5,g} \; {}_{c}T_{6,g,q} \right) \tag{22} $$

The second term provides the geometric stiffness associated with the Wagner effect, where $({}_{s}f_{5,g})$ is the Wagner stress resultant at Gauss point (g).

ELASTO-PLASTICITY

The determination of the local element response in the previous section necessitates the calculation, for each of the monitoring areas, of stress components (σ_x, ψ) from given strain components (ε_x, ξ). Within each monitoring area, the ensemble of fibres is assumed to be either elastic or, corporately, fully plastic; therefore, the elastic response, as well as the plastic interaction between the two stress components, must be specified. Since (ψ) is a generalised stress representing a twisting moment per unit area, the elastic modulus relating (ψ) to (ξ), as well as the plastic interaction between (σ_x) and (ψ), must be established from the distribution of shear stresses and strains over the monitoring area.

In the elastic range, the shear stress $(\tau_{x\hat{y}})$ is assumed to vary linearly over a monitoring area, as shown in Figs. 7.a-b, with the shear strain $(\gamma_{x\hat{y}})$ also varying linearly according to (6). Therefore, the elastic modulus relating (ψ) to (ξ) can be established from the equivalence of virtual work:

$$\psi\, A_m\, \delta\xi = \int_{A_m} \tau_{x\hat{y}}\, \delta\gamma_{x\hat{y}}\, dA = \int_{A_m} G(-2\hat{z}\xi)\delta(-2\hat{z}\xi)\, dA \Rightarrow$$

$$\psi = 4\hat{z}_e^2\, G\, \xi \tag{26.a}$$

where,

$$\hat{z}_e^2 = \frac{\int_{A_m} \hat{z}^2\, dA}{A_m} \tag{26.b}$$

Therefore, the response of a monitoring area is governed by the following relationship between the increment of stress and the increment of elastic strain:

$$\begin{Bmatrix} \Delta\sigma_x \\ \Delta\psi \end{Bmatrix} = E \begin{Bmatrix} \Delta\varepsilon_x^e \\ \Delta\xi^e \end{Bmatrix} \tag{27.a}$$

in which,

$$E = \begin{bmatrix} E & 0 \\ 0 & 4\hat{z}_e^2 G \end{bmatrix} \tag{27.b}$$

where, (E) is Young's elastic modulus, and (G) is the elastic shear modulus.

In the fully plastic range, the shear stress ($\tau_{x\hat{y}}$) is assumed to be constant over the monitoring area, as shown in Fig. 7.a. Therefore, applying the equivalence of virtual work, (ψ) can be related to ($\tau_{x\hat{y}}$) as follows:

$$\psi\, A_m\, \delta\xi = \int_{A_m} \tau_{x\hat{y}}\, \delta\gamma_{x\hat{y}}\, dA = \int_{A_m} \tau_{x\hat{y}}\, \delta(-2\hat{z}\,\xi)\, dA \Rightarrow$$

$$\tau_{x\hat{y}} = -\frac{\psi}{2\hat{z}_p} \tag{28.a}$$

where,

$$\hat{z}_p = \frac{\int_{A_m} \hat{z}\, dA}{A_m} \tag{28.b}$$

If the plate mid-plane passes through the monitoring area (Fig. 7.b), it may be shown that ($\hat{z}_p$) becomes:

$$\hat{z}_p = \frac{\int_{A_m} |\hat{z}|\, dA}{A_m} \tag{28.c}$$

The plastic interaction between material stresses ($\sigma_x, \tau_{x\hat{y}}$) can now be expressed as one between (σ_x, ψ), given the relationships in (28).

It is worth noting that the proposed replacement of shear stresses and strains by twist generalised stresses and strains allows as few as one monitoring area to be used over the plate thickness. In fact, such a coarse discretisation of the plate thickness leads to the exact elastic torsional stiffness, and results in only slight inaccuracies in the evaluation of plasticity effects.

The stress state (σ_x, ψ) corresponding to a strain state (ε_x, ξ) is established incrementally from the values at the last equilibrium step. Denoting these previous strain and stress states by (ε_x^o, ξ^o) and (σ_x^o, ψ^o), respectively, the current stress state (σ_x, ψ) corresponding to a strain increment $(\Delta\varepsilon_x, \Delta\xi)$ can be determined from the material stress-strain law.

Residual stresses are modelled by introducing non-zero values of (σ_x^o, ψ^o) for which the strains (ε_x^o, ξ^o) are zero at the start of analysis; i.e. the initial equilibrium state. In this work, only normal residual stresses are included, and a piecewise parabolic variation can be assumed over the plate width.

In the following sections, implementation details of the von Mises yield condition are presented; and, for comparison purposes, both isotropic and kinematic strain-hardening effects are considered. While the two models generally differ in the prediction of biaxial response and cyclic plasticity, they are both based on the same trilinear curve for the uniaxial monotonic response, as shown in Fig. 8.

Isotropic Strain-Hardening

The von Mises yield condition, involving interaction between (σ_x) and (ψ), can be expressed for the isotropic strain-hardening case by the following equation:

$$f(\sigma_x, \psi, \varepsilon_{ps}) = \sqrt{\sigma_x^2 + \frac{3}{4\hat{z}_p^2}\psi^2} - \sigma_o = 0 \qquad (29)$$

where,

σ_o : current value of uniaxial yield stress, dependent on accumulated equivalent plastic strain (ε_{ps}).

If the elastic application of the current increment of strain $(\Delta\varepsilon_x, \Delta\xi)$ should lead to a stress state (σ_x^e, ψ^e) which traverses the yield surface, then plastic strains $(\Delta\varepsilon_x^p, \Delta\xi^p)$ must be introduced in accordance with the associated flow rule to bring the stress state back to the yield surface. The one-step backward Euler procedure (Crisfield, 1991), illustrated in Fig. 9, is

adopted in virtue of its efficiency and the fact that it results in a symmetric consistent tangent modulus matrix ($_tE$). Accordingly, the current stress state (σ_x, ψ) must satisfy (29) where:

$$\begin{Bmatrix} \sigma_x \\ \psi \end{Bmatrix} = \begin{Bmatrix} \sigma_x^o \\ \psi^o \end{Bmatrix} + E\left(\begin{Bmatrix} \Delta\varepsilon_x \\ \Delta\xi \end{Bmatrix} - \begin{Bmatrix} \Delta\varepsilon_x^p \\ \Delta\xi^p \end{Bmatrix} \right) = \begin{Bmatrix} \sigma_x^o \\ \psi^o \end{Bmatrix} + E\left(\begin{Bmatrix} \Delta\varepsilon_x \\ \Delta\xi \end{Bmatrix} - \Delta\lambda N \right) \Rightarrow$$

$$\begin{Bmatrix} \sigma_x \\ \psi \end{Bmatrix} = \begin{Bmatrix} \sigma_x^e \\ \psi^e \end{Bmatrix} - \Delta\lambda\, E\, N \tag{30.a}$$

in which,

$$\begin{Bmatrix} \sigma_x^e \\ \psi^e \end{Bmatrix} = \begin{Bmatrix} \sigma_x^o \\ \psi^o \end{Bmatrix} + E\begin{Bmatrix} \Delta\varepsilon_x \\ \Delta\xi \end{Bmatrix} \tag{30.b}$$

$$N = \begin{Bmatrix} \dfrac{\partial f}{\partial \sigma_x} \\ \dfrac{\partial f}{\partial \psi} \end{Bmatrix} = \begin{Bmatrix} \dfrac{\sigma_x}{\sigma_o} \\ \dfrac{3\psi}{4\hat{z}_p^2 \sigma_o} \end{Bmatrix} \tag{30.c}$$

and,

$\Delta\lambda$: positive multiplier for incremental plastic strain

E : matrix of elastic properties given by (27).

It can also be shown that the increment of equivalent plastic strain $(\Delta\varepsilon_{ps})$ is identical to $(\Delta\lambda)$ (e.g. Crisfield, 1991), and hence the current yield stress (σ_o) appearing in (29) and (30) is determined, according to Fig. 8, from the following:

$$\sigma_o = \begin{cases} \sigma_y & , \text{ if } \lambda^o + \Delta\lambda \le \varepsilon_h \\ \sigma_o^o + H'\Delta\lambda & , \text{ if } \lambda^o \ge \varepsilon_h \\ \sigma_y + H'(\lambda^o + \Delta\lambda - \varepsilon_h) & , \text{ if } \varepsilon_h - \Delta\lambda \le \lambda^o \le \varepsilon_h \end{cases} \tag{31}$$

Equations (29) and (30) provide a nonlinear system of three simultaneous equations from which the current stress state (σ_x, ψ) and the multiplier $(\Delta\lambda)$ can be obtained. This nonlinear system of equations can be solved using a Newton-Raphson iterative strategy, where the values of (σ_x, ψ), (σ_o) and $(\Delta\lambda)$ are initialised to (σ_x^e, ψ^e), (σ_o^o) and zero, respectively. It is noted that if (σ_x^e, ψ^e) lies within the yield surface then the actual response is elastic, and (σ_x, ψ) is identical to (σ_x^e, ψ^e), with (σ_o) remaining unchanged and $(\Delta\lambda)$ taken as zero. Once structural equilibrium for the current step is achieved, the values of (σ_x^o, ψ^o), (σ_o^o) and (λ^o) are updated to (σ_x, ψ), (σ_o) and $(\lambda^o + \Delta\lambda)$.

The consistent tangent modulus matrix $({}_tE)$, needed in (22), is identical to (E) if the current stress increment is elastic; otherwise, $({}_tE)$ can be obtained from the following expression:

$$ {}_tE = R^{-1}E\left(I - \frac{\beta N\ N^T R^{-1} E}{\beta N^T\ R^{-1} E\, N + a}\right) \tag{32.a} $$

where,

$$ R = \begin{bmatrix} 1 + \dfrac{E\,\Delta\lambda}{\sigma_o} & 0 \\ 0 & 1 + \dfrac{3\hat{z}_e^2\, G\,\Delta\lambda}{\hat{z}_p^2\,\sigma_o} \end{bmatrix} \tag{32.b} $$

$$ \beta = \frac{\sigma_o^o}{\sigma_o} \tag{32.c} $$

$$ a = \begin{cases} 0 & , \text{if } \lambda^o + \Delta\lambda \le \varepsilon_h \\ H' & , \text{if } \lambda^o + \Delta\lambda > \varepsilon_h \end{cases} \tag{32.d} $$

and (I) is a (2×2) identity matrix.

Kinematic Strain-Hardening

Kinematic strain-hardening, which provides a more realistic representation of the hardening of steel than isotropic hardening, is associated with translation, rather than expansion, of the

yield surface. Denoting the current centre of this surface by (σ_{xc},ψ_c), as shown in Fig. 10, the von Mises yield criterion can be expressed as:

$$f(\sigma_x,\psi,\varepsilon_{ps}) = \sqrt{(\sigma_x-\sigma_{xc})^2 + \frac{3}{4\hat{z}_p^2}(\psi-\psi_c)^2} - \sigma_y = 0 \tag{33}$$

where,

σ_y : initial uniaxial yield stress

σ_{xc},ψ_c : current centre of yield surface, dependent on accumulated equivalent plastic strain (ε_{ps}).

As for isotropic hardening, if the elastic application of the current increment of strain $(\Delta\varepsilon_x,\Delta\xi)$ leads to a stress state (σ_x^e,ψ^e) which traverses the yield surface, plastic strains $(\Delta\varepsilon_x^p,\Delta\xi^p)$ are introduced using the one-step backward Euler procedure, as illustrated in Fig. 10. The centre of the yield surface translates in the radial direction (Ziegler, 1959) defined by the current stress state, as given by:

$$\begin{Bmatrix}\sigma_{xc}-\sigma_{xc}^o\\ \psi_c-\psi_c^o\end{Bmatrix} = \frac{\Delta r}{\sigma_y}\begin{Bmatrix}\sigma_x-\sigma_{xc}\\ \psi-\psi_c\end{Bmatrix} \Rightarrow$$

$$\begin{Bmatrix}\sigma_{xc}\\ \psi_c\end{Bmatrix} = \frac{1}{1+\frac{\Delta r}{\sigma_y}}\left(\begin{Bmatrix}\sigma_{xc}^o\\ \psi_c^o\end{Bmatrix} + \frac{\Delta r}{\sigma_y}\begin{Bmatrix}\sigma_x\\ \psi\end{Bmatrix}\right) \tag{34}$$

where,

$$\Delta r = \begin{cases} 0 & \text{, if } \varepsilon_{ps} \le \varepsilon_h \\ H'(\varepsilon_{ps}-\varepsilon_h) & \text{, if } \varepsilon_{ps} > \varepsilon_h \end{cases} \tag{35}$$

Substituting (34) in (33), the dependence on the equivalent plastic strain becomes restricted to the translation factor (Δr), resulting in a simplified yield condition:

$$f(\sigma_x,\psi,\varepsilon_{ps}) = \sqrt{(\sigma_x - \sigma_{xc}^o)^2 + \frac{3}{4\hat{z}_p^2}(\psi - \psi_c^o)^2} - (\sigma_y + \Delta r) = 0 \tag{36}$$

The current stress state (σ_x,ψ) can be related to the elastic stress state (σ_x^e,ψ^e) and the multiplier for plastic strains $(\Delta\lambda)$ in an identical manner to isotropic hardening, with a different normal vector (N):

$$\begin{Bmatrix}\sigma_x\\ \psi\end{Bmatrix} = \begin{Bmatrix}\sigma_x^e\\ \psi^e\end{Bmatrix} - \Delta\lambda\, E\, N \tag{37.a}$$

in which,

$$\begin{Bmatrix}\sigma_x^e\\ \psi^e\end{Bmatrix} = \begin{Bmatrix}\sigma_x^o\\ \psi^o\end{Bmatrix} + E\begin{Bmatrix}\Delta\varepsilon_x\\ \Delta\xi\end{Bmatrix} \tag{37.b}$$

$$N = \begin{Bmatrix}\frac{\partial f}{\partial \sigma_x}\\ \frac{\partial f}{\partial \psi}\end{Bmatrix} = \begin{Bmatrix}\frac{\sigma_x - \sigma_{xc}^o}{\sigma_y + \Delta r}\\ \frac{3(\psi - \psi_c^o)}{4\hat{z}_p^2(\sigma_y + \Delta r)}\end{Bmatrix} \tag{37.c}$$

Again, considering that the increment of equivalent plastic strain $(\Delta\varepsilon_{ps})$ is identical to $(\Delta\lambda)$, the incremental translation coefficient (Δr) appearing in (36) and (37) is determined according to the following:

$$\Delta r = \begin{cases} 0 & \text{, if } \lambda^o + \Delta\lambda \le \varepsilon_h \\ H'\Delta\lambda & \text{, if } \lambda^o \ge \varepsilon_h \\ H'(\lambda^o + \Delta\lambda - \varepsilon_h) & \text{, if } \varepsilon_h - \Delta\lambda \le \lambda^o \le \varepsilon_h \end{cases} \tag{38}$$

The nonlinear system of three simultaneous equations given by (36) and (37) can be solved iteratively using a Newton-Raphson strategy, through which (σ_x,ψ), $(\Delta\lambda)$, (Δr) and hence (σ_{xc},ψ_c) can be established. Once structural equilibrium for the current step is achieved, the values of (σ_x^o,ψ^o), (σ_{xc}^o,ψ_c^o) and (λ^o) are updated to (σ_x,ψ), (σ_{xc},ψ_c) and $(\lambda^o + \Delta\lambda)$.

The consistent tangent modulus matrix $({}_tE)$ is identical to that obtained for the isotropic strain-hardening case in (32), but with different (β) and (R):

$$R = \begin{bmatrix} 1 + \dfrac{E\Delta\lambda}{\sigma_y + \Delta r} & 0 \\ 0 & 1 + \dfrac{3\hat{z}_e^2 G\Delta\lambda}{\hat{z}_p^2(\sigma_y + \Delta r)} \end{bmatrix} \tag{39.a}$$

$$\beta = \frac{\sigma_y}{\sigma_y + \Delta r} \tag{39.b}$$

It is worth noting that for both cases of isotropic and kinematic hardening, the consistent tangent modulus matrix $({}_tE)$ is symmetric.

GLOBAL ANALYSIS

The derivation of the proposed elasto-plastic cubic element in a local Eulerian system provides considerable formulation advantages. However, the use of this formulation within a global analysis capability requires transformations between the local Eulerian system and a global reference system common to all elements of the structure. In this regard, the proposed formulation is implemented within a large displacement Eulerian approach for thin-walled frames (Izzuddin, 1995), where three transformations are required between the Eulerian and global systems (Izzuddin, 1991; Izzuddin and Elnashai, 1993-a). The first is a transformation of global displacements to local Eulerian displacements $({}_cu)$. The second is a transformation of local Eulerian forces $({}_cf)$ to global forces. Finally, the third is a transformation of local Eulerian tangent stiffness $({}_ck)$ to global tangent stiffness.

The above transformations enable the calculation of global element forces, given a set of global element displacements, and allow the determination of a global element tangent stiffness matrix. Therefore, using standard assembly procedures, the overall structural resistance can be established from the structural displacements, and a structural tangent stiffness matrix can be obtained. Hence, the solution of the nonlinear governing equations for

the structural system can be performed for the current increment using iterative solution strategies, such as the Newton-Raphson procedure. In this context, it should be noted that the evaluation of the current stress state for the various monitoring areas must be undertaken with reference to the stress state at the end of the last equilibrium step, and not that corresponding to the previous iteration.

CONCLUSION

This paper presents a new one-dimensional formulation for the large displacement analysis of elasto-plastic frames with thin-walled open member cross-sections. It accounts for initial imperfections, residual stresses, the Wagner effect and yielding governed by interacting shear and normal stresses. The proposed formulation is derived in a local Eulerian system. This allows the use of simplified strain-displacement relationships in the local system without compromising the accuracy of modelling nonlinearities in the global response due to axial-flexural-torsional coupling. Consequently, the formulation can be used to model the elasto-plastic response of thin-walled frames subject to flexural and lateral torsional instability.

In the local system, the formulation employs eight freedoms with the centroidal axis chosen as the element reference line. Four reference line displacements define the strain state over the element, cubic shape functions being used for the transverse displacements and angle of twist, and a linear shape function for the axial displacement. The local element response is obtained through the virtual work method, where the integration of the governing equations is performed numerically with the aid of two Gauss points along the element length and a number of monitoring areas over the cross-section. Whilst the formulation allows a variable number of monitoring areas to be used over the cross-section, only two Gauss points are employed along the element length. Although more Gauss points could be used over the element, this would demand excessive computational requirements without a commensurate improvement in accuracy, especially since several elements are required to model the nonlinear response of one member.

Over each cross-sectional monitoring area, the strain state is defined by a normal strain at the centre of the area and a rate of twist generalised strain, which allows a coarse discretisation over the thickness of cross-section component plates. The stress state, defined by the normal stress at the centre of the monitoring area and a generalised twisting moment per unit area, is obtained from the strain state using an elastic fully-plastic material law based on the von Mises criterion for interactive yielding between the two stress components. Implementation details for isotropic and kinematic strain-hardening are provided, where the backward Euler return to the interaction curve is employed.

The incorporation of the proposed formulation within an Eulerian large displacement approach is outlined, and the three necessary transformations between the Eulerian and global systems are described. The companion paper aims at verifying the accuracy of the new formulation, identifying the significance of the various assumptions made in its derivation, and providing some examples of its application to the elasto-plastic analysis of thin-walled members and frames.

REFERENCES

1. Allen, H.G. and Bulson, P.S., 1980. Background to Buckling, McGraw Hill Book Company, Ltd., London.

2. Barsoum, R.S. and Gallagher, R.H., 1970. "Finite Element Analysis of Torsional and Torsional-Flexural Stability Problems", International Journal for Numerical Methods in Engineering, Vol. 2, pp. 335-352.

3. Bazant, Z.P. and El Nimeiri, M., 1973. "Large-Deflection Spatial Buckling of Thin-Walled Beams and Frames", Journal of the Engineering Mechanics Division, ASCE, Vol. 99, No. EM6, pp. 1259-1281.

4. Bleich, F., 1952. Buckling Strength of Metal Structures, McGraw Hill Book Company, Inc., New York.

5. Chan, S.L. and Kitipornchai, S., 1987. "Geometric Nonlinear Analysis of Asymmetric Thin-Walled Beam-Columns", Engineering Structures, Vol. 9, pp. 243-254.

6. Chen, H. and Blandford, G.E., 1991. "Thin-Walled Space Frames. I: Large-Deformation Analysis Theory", Journal of Structural Engineering, ASCE, Vol. 117, No. 8, pp. 2499-2520.

7. Conci, A. and Gattass, M., 1990-a. "Natural Approach for Geometric Non-Linear Analysis of Thin-Walled Frames", International Journal for Numerical Methods in Engineering, Vol. 30, pp. 207-231.

8. Conci, A. and Gattass, M., 1990-b. "Natural Approach for Thin-Walled Beam-Columns with Elastic-Plasticity", International Journal for Numerical Methods in Engineering, Vol. 29, pp. 1653-1679.

9. Crisfield, M.A., 1991. Non-linear Finite Element Analysis of Solids and Structures, Volume 1, John Wiley & Sons, Chichester, England.

10. El-Zanaty, M.H. and Murray, D.W., 1983. "Nonlinear Finite Element Analysis of Steel Frames", Journal of Structural Engineering, ASCE, Vol. 109, No. 2, pp. 353-368.

11. Epstein, M., Nixon, D. and Murray, W., 1978. "Large Displacement Inelastic Analysis of Beam-Columns", Journal of the Structural Division, ASCE, Vol. 104, ST5, 841-853.

12. Goto, Y. and Chen, W.F., 1989. "On the Validity of Wagner Hypothesis", International Journal of Solids and Structures, Vol. 25, No. 6, pp. 621-634.

13. Hasegawa, A., Liyanage, K.K., Noda, M. and Nishino, F., 1987. "An Inelastic Finite Displacement Formulation of Thin-Walled Members", Structural Engineering/Earthquake Engineering, Vol. 4, No. 2, pp. 269-276.

14. Izzuddin, B.A. and Elnashai, A.S., 1993-a. "Eulerian Formulation for Large Displacement Analysis of Space Frames". Journal of Engineering Mechanics, ASCE, Vol. 119, No. 3, pp. 549-569.

15. Izzuddin, B.A. and Elnashai, A.S., 1993-b. "Adaptive Space Frame Analysis: Part II, A Distributed Plasticity Approach", Structures and Buildings Journal, Proceedings of the Institution of Civil Engineers, Vol. 99, No. 3, pp. 317-326.

16. Izzuddin, B.A. and Lloyd Smith, D., 1995. "Large Displacement Analysis of Inelastic Thin-Walled Frames. Part II: Verification and Application", Companion paper.

17. Izzuddin, B.A., 1991. "Nonlinear Dynamic Analysis of Framed Structures", Thesis submitted for the degree of Doctor of Philosophy in the University of London, Department of Civil Engineering, Imperial College, London.

18. Izzuddin, B.A., 1995. "An Eulerian Approach to the Large Displacement Analysis of Thin-Walled Frames", Proceedings of the Institution of Civil Engineers, U.K., Vol. 110, No. 1, pp. 50-65.

19. Mallet, R.H. and Marcal, P.V., 1968. "Finite Element Analysis of Nonlinear Structures", Journal of the Structural Division, ASCE, Vol. 94, No. ST9, pp. 2081-2105.

20. Meek, J.L. and Lin, W.J., 1990. "Geometric and Material Non-Linear Analysis of Thin-Walled Beam-Columns", Journal of Structural Engineering, ASCE, Vol. 116, No. 6, pp. 1473-1490.

21. Meek, J.L. and Loganathan, S., 1990. "Geometric and Material Non-Linear Behaviour of Beam-Columns", Computers & Structures, Vol. 34, No. 1, pp. 87-100.

22. Nethercot, D.A., 1975. "Inelastic Buckling of Steel Beams under Non-Uniform Moment", The Structural Engineer, Vol. 53, No. 2, pp. 73-78.

23. Oran, C., 1973. "Tangent Stiffness in Space Frames", Journal of the Structural Division, ASCE, Vol. 99, No. ST6, pp. 987-1001.

24. Pi, Y.L. and Trahair, N.S., 1992. "Prebuckling Deflections and Lateral Buckling. I: Theory" Journal of Structural Engineering, ASCE, Vol. 118, No. 11, 2949-2985.

25. Pi, Y.L. and Trahair, N.S., 1994. "Nonlinear Inelastic Analysis of Steel Beam-Columns. I: Theory", Journal of Structural Engineering, ASCE, Vol. 120, No. 7, pp. 2041-2061.

26. Trahair, N.S. and Kitipornchai, S., 1972. "Buckling of Inelastic I-Beams under Uniform Moment", Journal of the Structural Division, ASCE, Vol. 98, No. ST11, pp. 2551-2566.

27. Wen, R.K. and Rahimzadeh, J., 1983. "Nonlinear Elastic Frame Analysis by Finite Element", Journal of Structural Engineering, ASCE, Vol. 109, No. 8, pp. 1952-1971.

28. Ziegler, H., 1959. "A Modification of Prager's Hardening Rule", Quarterly of Applied Mathematics, Vol. 17, No. 1, pp. 55-65.

APPENDIX A: ARRAY $\boxed{{}_{c}T}$

Array $({}_{c}T)$ required in (19) and (21) is a (6×2×8) array representing the weighted first derivatives of generalised strains with respect to local displacements, and is given by:

$$ {}_{c}T_{j,g,k} = \left(\frac{L}{2}\right)\left(\frac{\partial_s u_{j,g}}{\partial_c u_k}\right) \tag{40.a} $$

$$ {}_{c}T_1 = \frac{1}{2}\begin{bmatrix} 0 & 0 & 0 & 0 & 1 & 0 & 0 & 0 \\ 0 & 0 & 0 & 0 & 1 & 0 & 0 & 0 \end{bmatrix} \tag{40.b} $$

$$ {}_{c}T_2 = \frac{1}{2}\begin{bmatrix} -c_1 & -\alpha_1^i c_1 & -c_2 & -\alpha_1^i c_2 & 0 & 0 & 0 & 0 \\ c_2 & \alpha_2^i c_2 & c_1 & \alpha_2^i c_1 & 0 & 0 & 0 & 0 \end{bmatrix} \tag{40.c} $$

$$ {}_{c}T_3 = \frac{1}{2}\begin{bmatrix} \alpha_1^i c_1 & -c_1 & \alpha_1^i c_2 & -c_2 & 0 & 0 & 0 & 0 \\ -\alpha_2^i c_2 & c_2 & -\alpha_2^i c_1 & c_1 & 0 & 0 & 0 & 0 \end{bmatrix} \tag{40.d} $$

$$ {}_{c}T_4 = \frac{1}{2}\begin{bmatrix} 0 & 0 & 0 & 0 & 0 & c_3 & -c_1 & -c_2 \\ 0 & 0 & 0 & 0 & 0 & -c_3 & c_2 & c_1 \end{bmatrix} \tag{40.e} $$

$$ {}_{c}T_5 = \begin{bmatrix} \alpha_1'^i + \alpha_1' & 0 \\ 0 & \alpha_2'^i + \alpha_2' \end{bmatrix} {}_{c}T_6 \tag{40.f} $$

$$ {}_{c}T_6 = \frac{1}{2}\begin{bmatrix} 0 & 0 & 0 & 0 & 0 & 1 & 1/c_3 & -1/c_3 \\ 0 & 0 & 0 & 0 & 0 & 1 & -1/c_3 & 1/c_3 \end{bmatrix} \tag{40.g} $$

where,

$$ c_1 = \sqrt{3} + 1 \tag{41.a} $$

$$ c_2 = \sqrt{3} - 1 \tag{41.b} $$

$$ c_3 = \frac{2\sqrt{3}}{L} \tag{41.c} $$

$$\alpha_1^i = \alpha_g^i({}_g x_1) \tag{41.d}$$

$$\alpha_2^i = \alpha_g^i({}_g x_2) \tag{41.e}$$

$$\alpha_1'^i = \alpha_g'^i({}_g x_1) \tag{41.f}$$

$$\alpha_2'^i = \alpha_g'^i({}_g x_2) \tag{41.g}$$

$$\alpha_1' = \alpha_g'({}_g x_1) \tag{41.h}$$

$$\alpha_2' = \alpha_g'({}_g x_2) \tag{41.i}$$

APPENDIX B: NOTATION

- Generic symbols of arrays, matrices and vectors are represented by **bold** font-type and can include left side subscripts and superscripts (e.g. ${}_{c}\mathbf{u}$, ${}_{s}\mathbf{f}$).

- Subscripts and superscripts to the right side of the generic symbol indicate the term of the array, matrix or vector under consideration (e.g. ${}_{c}\mathbf{u}_{i}$, ${}_{s}\mathbf{f}_{5,1}$).

Operators

$f'(x)$: first derivative of f(x) with respect to (x).

$f''(x)$: second derivative of f(x) with respect to (x).

^{T} : right-side superscript, transpose sign.

∂ : partial differentiation.

δ : infinitesimal increment.

Δ : finite increment.

^{o} : right side superscript indicating values at end of previous incremental step.

$[\ ]$: encloses terms of a matrix.

$\langle\ \rangle$: encloses terms of a row vector.

$\{\ \}$: encloses terms of a column vector.

Symbols

A : cross-sectional area.

A : vector of monitoring areas.

d : array of distances and warping function values for monitoring areas.

E : elastic Young's modulus.

e : array of monitoring area strains.

$\mathbf{E}$: elastic modulus matrix.

${}_t\mathbf{E}$: tangent modulus matrix.

${}_c\mathbf{f}$: local element forces

$$\left\langle M_{1y}, M_{1z}, M_{2y}, M_{2z}, F, M_T, B_1, B_2 \right\rangle^T .$$

${}_s\mathbf{f}$: cross-sectional generalised forces.

G : elastic shear modulus.

H' : strain-hardening parameter.

${}_c\mathbf{k}$: local element tangent stiffness matrix.

${}_s\mathbf{k}$: cross-sectional generalised tangent stiffness.

L : element length.

n : number of monitoring areas.

$\mathbf{N}$: normal vector to interaction curve.

$\mathbf{s}$: array of monitoring area stresses.

${}_c\mathbf{T}$: transformation matrix given in Appendix A.

u : cross-sectional axial displacement.

u_g : reference line displacement in x-direction.

${}_c\mathbf{u}$: local element freedoms

$$\left\langle \theta_{1y}, \theta_{1z}, \theta_{2y}, \theta_{2z}, \Delta, \theta_T, \theta_1', \theta_2' \right\rangle^T .$$

${}_s\mathbf{u}$: cross-sectional generalised strains.

v : transverse displacement over cross-section.

v_g : reference line displacement in $\bar{y}$-direction.

v^i : cross-sectional transverse displacement due to twist imperfection.

$\hat{v}$: transverse in-plane displacement over component plate.

w : transverse displacement over cross-section.

w_g : reference line displacement in $\bar{z}$-direction.

w^i : cross-sectional transverse displacement due to twist imperfection.

x : reference coordinate along element length.

$_gx$: vector of coordinates of two Gauss points.

y : reference coordinate over cross-section.

$\bar{y}$: reference coordinate over cross-section subject to twist imperfection.

$\hat{y}$: local reference coordinate along component plate.

$\mathbf{y}$: array of coordinates (y) for monitoring areas.

z : reference coordinate over cross-section.

$\bar{z}$: reference coordinate over cross-section subject to twist imperfection.

$\hat{z}$: local reference coordinate across component plate.

$\hat{z}_e$: equivalent elastic twist arm of monitoring area.

$\hat{z}_p$: equivalent plastic twist arm of monitoring area.

$\mathbf{z}$: array of coordinates (z) for monitoring areas.

α_g : reference line angle of twist.

α_g^i : reference line twist imperfection.

Δr : factor for interaction curve translation.

ε_h : limit equivalent plastic strain for strain-hardening.

ε_{ps} : equivalent plastic strain.

ε_x : normal strain.

Φ : warping function of (y,z).

$\mathbf{\Phi}$: array of warping function values (Φ) for monitoring areas.

$\gamma_{x\hat{y}}$: in-plane shear strain over component plate.

λ : positive multiplier for plastic strains.

θ_1^i, θ_2^i : twist imperfections at nodes (1) and (2).

$\theta_1'^i, \theta_2'^i$: rates of twist imperfection at nodes (1) and (2).

σ_o : uniaxial yield stress.

σ_x : normal stress.

σ_{xc} : interaction curve centre abscissa.

σ_x^e : normal stress assuming elastic strain increment.

σ_y : initial yield stress.

$\tau_{x\hat{y}}$: in-plane shear stress over component plate.

ξ : rate of twist generalised strain.

ψ : rate of twist generalised stress.

ψ_c : interaction curve centre ordinate.

ψ^e : rate of twist generalised stress assuming elastic strain increment.

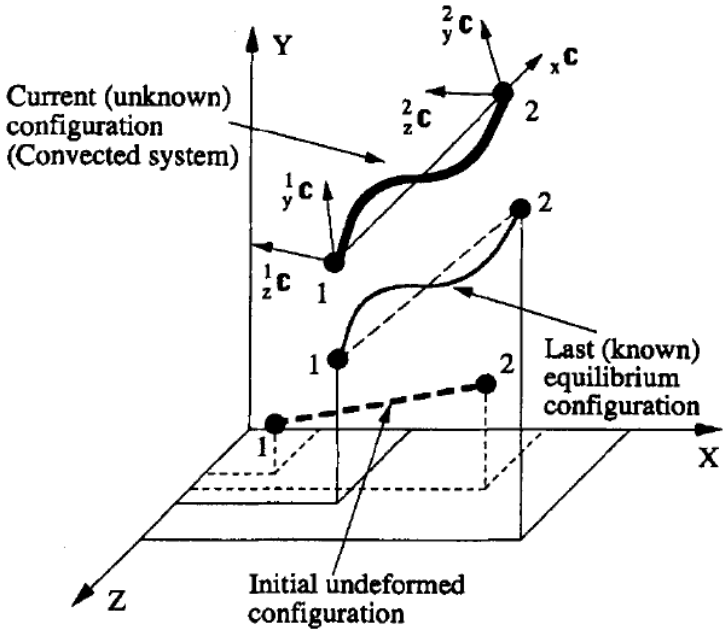

Fig. 1 Local Eulerian (convected) system

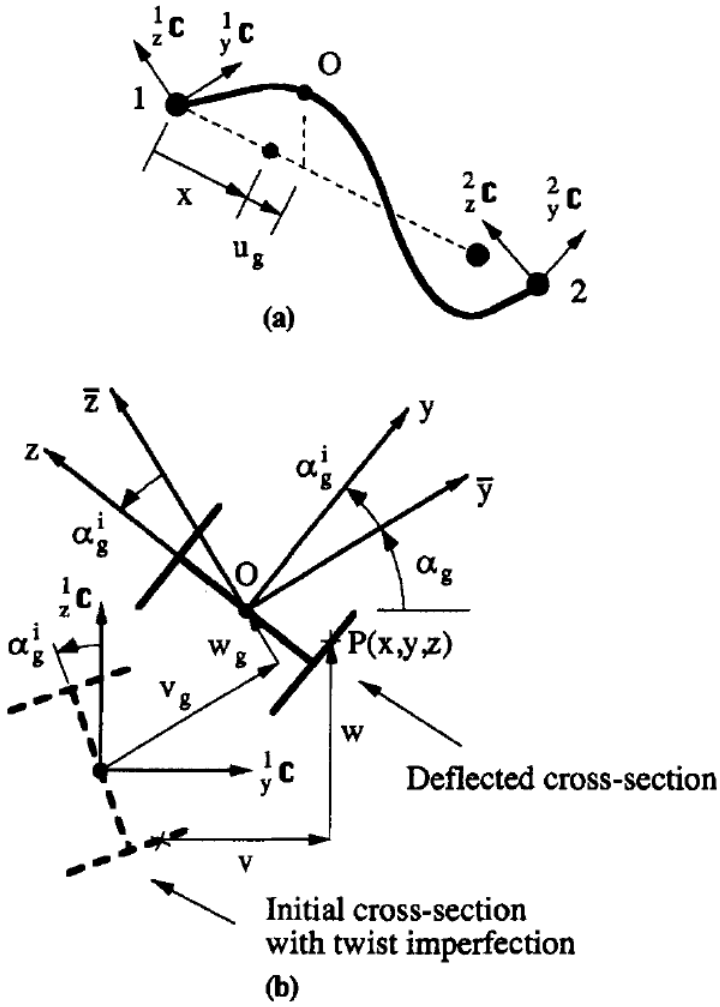

Fig. 2 Reference line displacements at position (x)

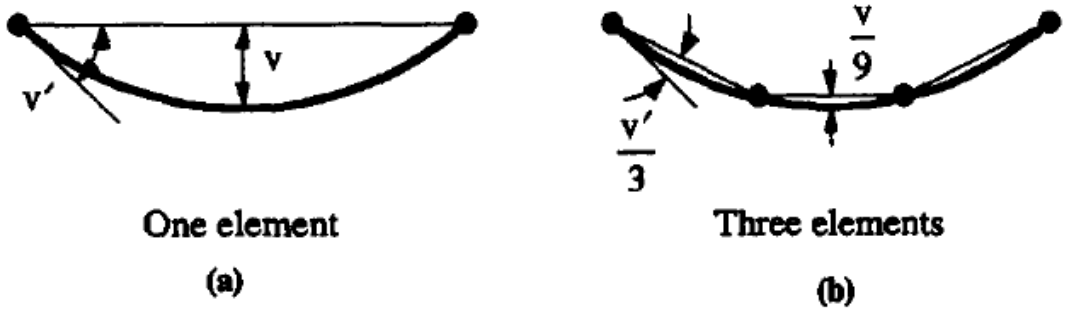

Fig. 3 Reduction of transverse displacement and its first derivative with elements

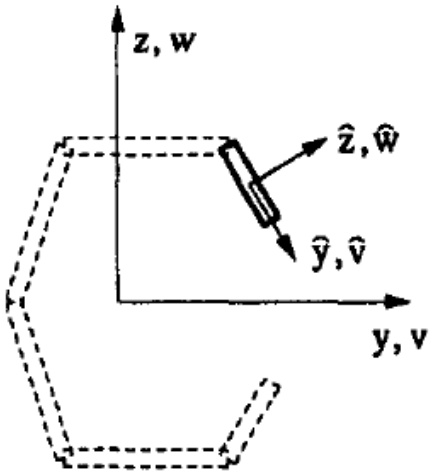

Fig. 4 Local reference system of a component plate

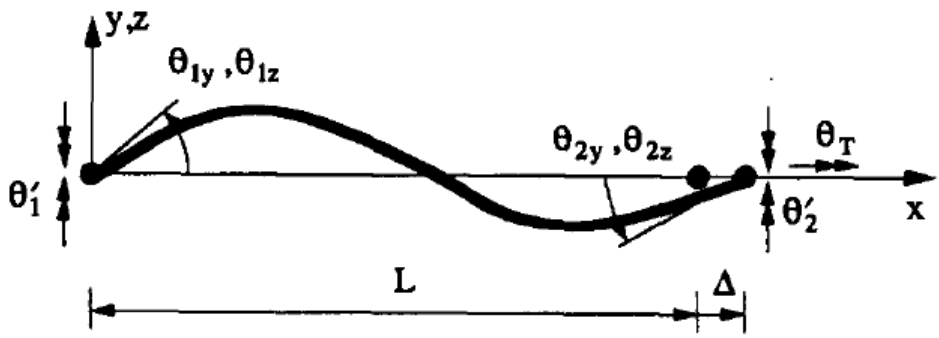

Fig. 5 Local freedoms of cubic formulation

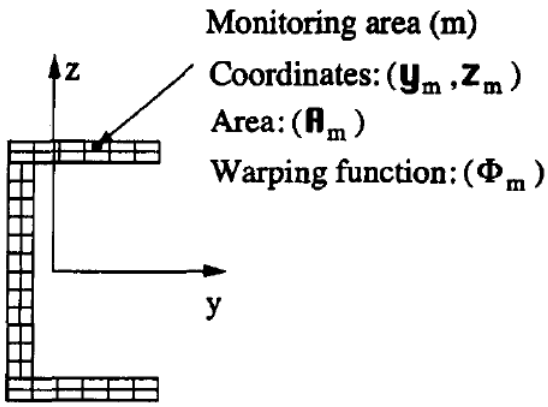

Fig. 6 Discretisation of a channel section into monitoring areas

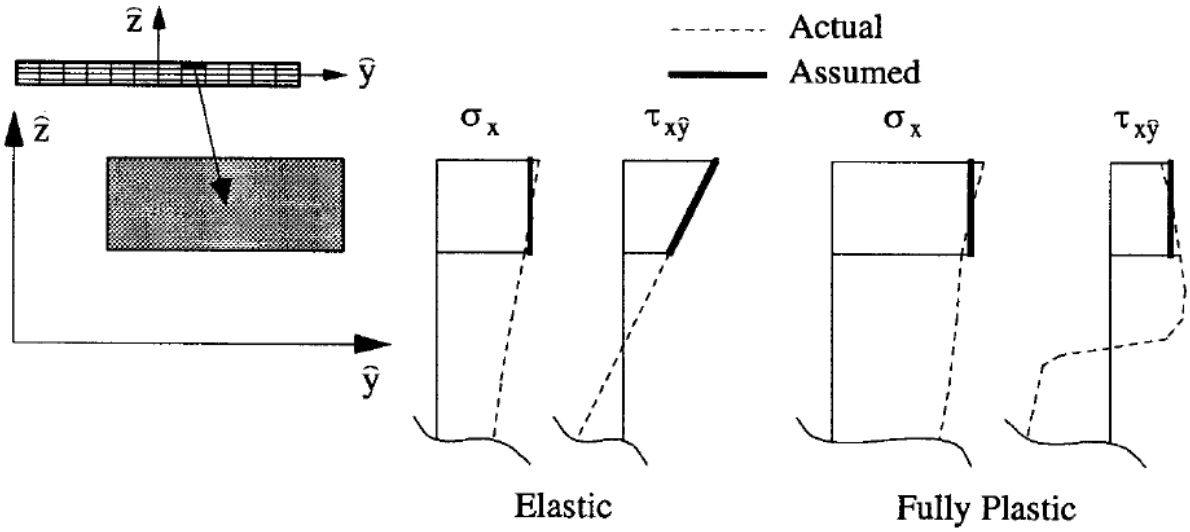

Fig. 7.a Distribution of stresses over monitoring area: Mid-plane outside monitoring area

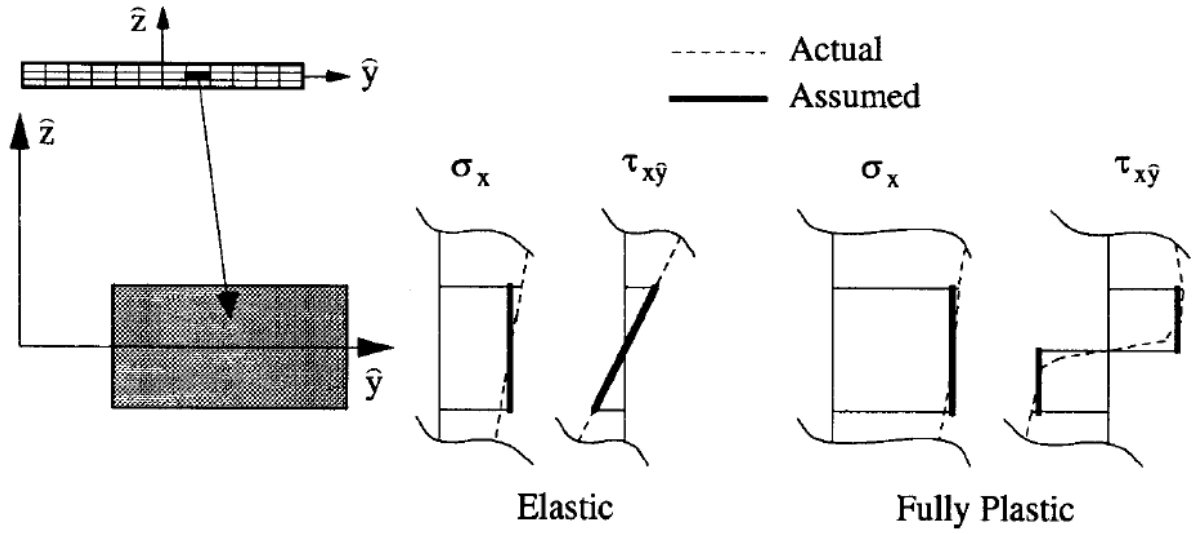

Fig. 7.b Distribution of stresses over monitoring area: Mid-plane crosses monitoring area

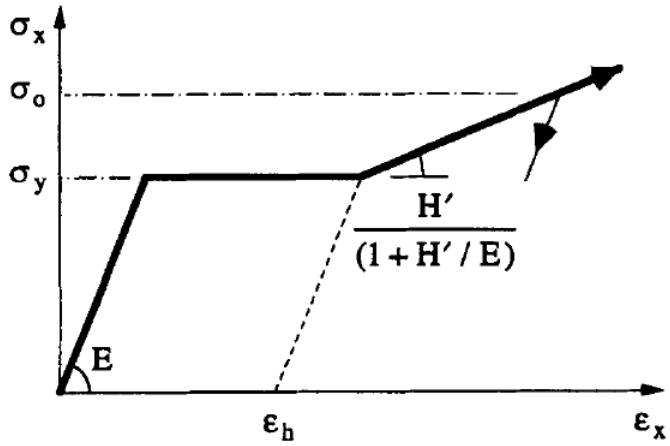

Fig. 8 Trilinear uniaxial stress-strain curve

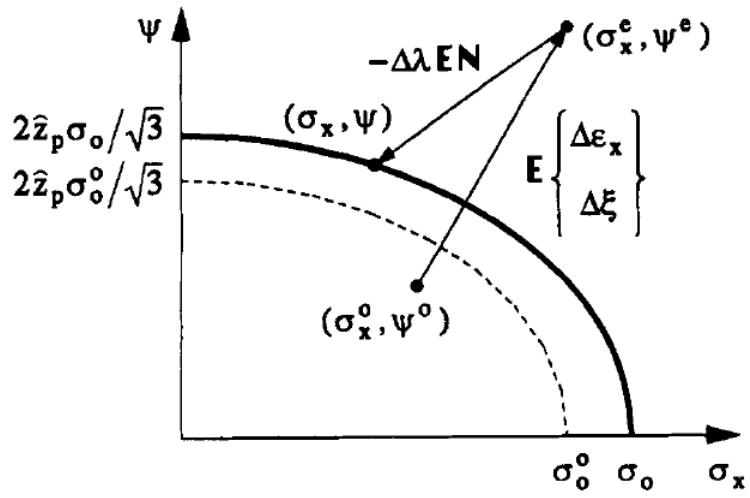

Fig. 9 Backward Euler return with isotropic hardening

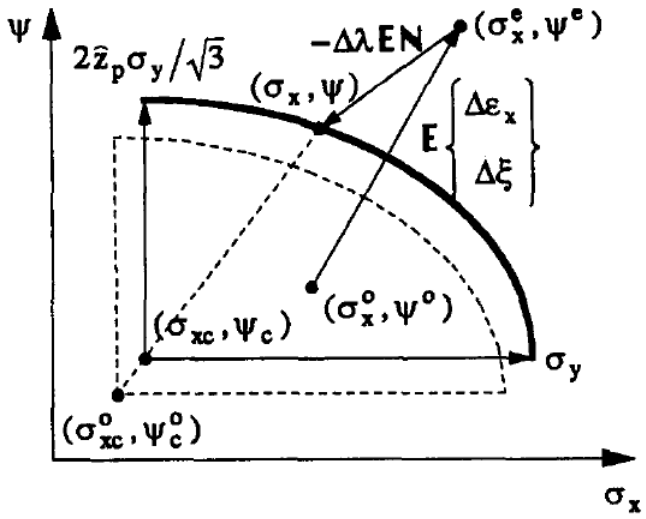

Fig. 10 Backward Euler return with kinematic hardening